Solubilities Inferred from the Combination of Experiment and Simulation. Case Study of Quercetin in a Variety of Solvents

Latifa Chebil,*,† Christophe Chipot,‡,§,∥ Fabien Archambault,‡ Catherine Humeau,† Jean Marc Engasser,† Mohamed Ghoul,† and François Dehez*,‡

Laboratoire d'ingénierie des biomolécules (LIBio), Nancy Université, 2 avenue de la forêt de Haye, 54500 Vandœuvre-lès-Nancy, France, Equipe de Dynamique des Assemblages Membranaires, UMR CNRS-UHP No. 7565, Nancy Université, BP 70239, 54506 Vandœuvre-lès-Nancy, France, and Theoretical and Computational Biophysics Group, Beckman Institute for Advanced Science and Engineering, University of Illinois at Urbana-Champaign, 405 North Mathews, Urbana, Illinois 61801

Received: May 19, 2010; Revised Manuscript Received: July 8, 2010

A strategy to infer solubilities from the combination of experiment and all-atom simulations is presented. From a single experimental estimate, the solubility of a substrate can be predicted in various environments from the related free energies of solvation. In the case of quercetin, the methodology was shown to reproduce the experimental solubilities in chloroform, water, acetonitrile, acetone, and *tert*-amyl alcohol within 0.5 log unit. The reliability of the estimates is markedly correlated to the accuracy of the experimental measure and to both the accuracy and precision of the computed free energies of solvation.

Introduction

Solubility is a physicochemical property of paramount importance in the formulation of new pharmaceutical compounds. Precise knowledge of solubility is highly desirable to predict the availability of a chemical species in the context of its absorption in vivo, or of a given substrate in the framework of an organic synthesis. Experimental determination of solubilities, however, constitutes a daunting and time-consuming endeavor when a large number of compounds and/or solvents are involved. In silico approaches, therefore, represent an appealing alternative to predict solubilities. Approximate quantitative structure−property relationship (QSPR) methods[1−3] have been widely employed to estimate this physicochemical quantity. When looking for generality and precision, more rigorous routes have, however, to be explored. The accurate computation of the solubility of a given chemical species requires the knowledge of the free-energy differences associated with its transfer in the solvent and its dissociation from the crystal. Determining in silico the latter quantity, nevertheless, remains somewhat cumbersome. In a series of recent articles, Lindfors and colleagues.[4−7] proposed a predictive model capable of estimating reasonably solubilities in water. For a variety of drugs, they computed, using all-atom Monte Carlo simulations, the free energy of solvation in pure melt at 673.17 K and the free energy associated with the supercooling of the melt from 673.17 to 298 K. Combination of these quantities with hydration free energies allows the solubility of amorphous drugs to be determined in water. In addition, the solubility of the crystal can be inferred from that of the amorphous solid on the basis of experimental melting data, viz., entropy and temperature of melting.

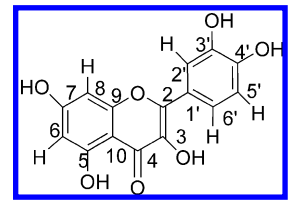

Figure 1. Molecular structure of quercetin.

Evaluation of the crystal contribution represents an equally difficult undertaking, which evidently cannot be performed routinely. Moreover, in the context of chemical synthesis, knowledge of the solubility is important not only in water but also in a variety of solvents that can be used to mediate chemical reactions. Here, a strategy is developed to infer the solubilities of a given compound in different environments by combining theory and experiment. Molecular dynamics simulations and free-energy perturbation (FEP) methodology[8] are employed to predict the relative free energies of solvation in a variety of solvents. It is shown that using these data together with a single experimental solubility measurement allows the full solubility scale to be determined with an appreciable accuracy. The methodology is illustrated in the case of quercetin (3,3′,4′,5,7-pentahydroxy flavone) (see Figure 1), one of the most studied members of the flavonoid family. This compound possesses a strong antioxidant activity, central in preventing the risk of cardiovascular, neurodegenerative, and cancer diseases.[9,10] It is an overall hydrophobic species, which needs to be modified to be incorporated efficiently in a chemical formulation. This alteration can be achieved by means of enzymatic catalysis, employing for instance immobilized *Pseudomonas cepacia* lipase in organic phases,[11] the effectiveness of the process being strongly dependent on the solubility of the substrate.[12]

* To whom correspondence should be addressed. L.C.: tel, +33-383596195; fax, +33-383595778; e-mail, Latifa.chebil@ensaia.inpl-nancy.fr. F.D.: tel, +33-383684098; fax, +33-383684387; e-mail, Francois.Dehez@srsmc.uhp.

† Laboratoire d'ingénierie des biomolécules (LIBio). E-mail: C.H., Catherine.Humeau@ensaia.inpl-nancy.fr; J.M.E., Jean-Marc.Engasser@ensaia.inpl-nancy.fr; M.G., Mohamed.Ghoul@ensaia.inpl-nancy.fr.

‡ Equipe de Dynamique des Assemblages Membranaires. E-mail: C.C, Christophe.Chipot@srsmc.uhp-nancy.fr; F.A., Fabien.Archambault@srsmc.uhp-nancy.fr.

§ University of Illinois at Urbana-Champaign.

∥ On leave from Équipe de dynamique des assemblages membranaires, UMR 7565, Nancy Université, BP 239, 54506 Vandoeuvre-lès-Nancy cedex, France.

10.1021/jp104569k
Published on Web 08/17/2010

Methodology

Molecular Models. The OPLS (optimized potential for liquid simulations) force field developed by Jorgensen and colleagues.[13] was used to describe all the solvents utilized in this work, e.g., water (TIP3P),[14] acetonitrile,[15,16] acetone,[17] and chloroform.[18] *tert*-Amyl alcohol was modeled using the *tert*-butyl alcohol OPLS parameters. For quercetin, all-atom OPLS parameters were used whenever available. For the C2−C1′ bond, a torsional potential was optimized in the spirit of the OPLS force field to reproduce the potential energy surface determined quantum-mechanically at the DFT (B3LYP)[19]/6-31G* level (see Supporting Information). This surface was obtained on the basis of the equilibrium geometry of quercetin, for which the dihedral angle O−C2−C1′−C6′ (φ) was varied by 10° increments. All quantum-chemical calculations were performed using Gaussian03.[20] The resulting torsional potential can be written

$$E(\varphi) = \frac{V_1}{2}[1 + \cos(\varphi)] + \frac{V_2}{2}[1 \cos(2\varphi)] \qquad (1)$$

with $V_1 = -0.40$ kcal/mol and $V_2 = 6.58$ kcal/mol.

The electrostatic fingerprint of quercetin was modeled by means of different sets of atomic charges to account in an average sense for the polarization due to the various environments. In practice, a grid of approximately 15 000 points (distributed spatially between envelopes corresponding to 2 and 4 times the van der Waals radii of the participating atoms) was built around the molecule. The electrostatic potential was evaluated at each point of the grid at the B3LYP/6-31G* level, employing a dielectric continuum representation of the different environments by means of the PCM model of solvation[21] (polarizable continuum model). In a final step, the OPEP[22] package was used to derive the atomic charges from the electrostatic potential maps (see Supporting Information).

Molecular Dynamics (MD) Simulations. For each environment, quercetin, either as a monomer or a dimer, was immersed in a pre-equilibrated cubic box containing approximately 500 explicit molecules of solvent. MD trajectories of 0.5 ns were performed to thermalize each system prior to a production run of 1.5 ns. All MD simulations were carried out using the NAMD package,[23] in the isobaric−isothermal ensemble. The temperature and the pressure were kept constant at 323 K and 1 atm using, respectively, Langevin dynamics and the Langevin piston method.[24] The particle mesh Ewald (PME) algorithm[25] was used to account for long-range electrostatic interactions. The equations of motion were integrated by means of a multiple-time-step algorithm[26] with a time step of 2 and 4 fs for short- and long-range interactions, respectively.

Free Energy and Solubility Calculations. The following strategy was used to compute the solvation free energies. Transfer of quercetin from the low-pressure gaseous phase to the bulk solvent was modeled by means of a double-annihilation[27] of the solute in the two environments, as illustrated in Figure 2.

The reaction pathway connecting the initial and the final states of the annihilation and creation transformations was stratified[28] in a series of 24 strata, or windows, of uneven widths. In each window, 4000 equilibration steps were generated prior to the production of 26 000 steps, over which the ensemble averages were calculated. This sampling strategy represents a total of 1.44 ns for each transformation. In addition to the use of strata of decreasing width toward the end points of the free-energy calculation, which constitutes an artificial and incomplete remedy to circumvent singularities in the van der Waals potential, a soft-core correction was introduced in the form of a separation-shifted scaling scheme[29] to prevent incoming particles from colliding with the surrounding solvent molecules.

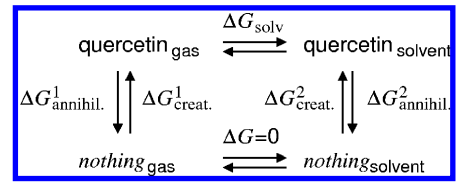

Figure 2. Solvation free energy, ΔG_{solv}, of quercetin measured from a double-annihilation scheme, whereby the interaction of the solute with its environment is progressively turned out, viz. $\Delta G_{solv} = \Delta G^1_{annihil} - \Delta G^2_{annihil}$, or turned on, viz. $\Delta G_{solv} = \Delta G^2_{creat} - \Delta G^1_{creat}$. In practice, neglect of perturbed intramolecular interactions obviates the need to compute the gas-phase contribution, $\Delta G^1_{annihil}$, to the solvation free energy, which is justified by the similarity of the atomic charges determined in the different solvents.

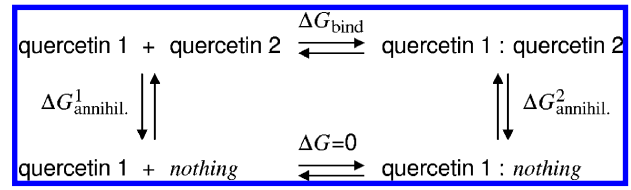

Figure 3. Binding free energy, ΔG_{bind}, of quercetin measured from a double-annihilation scheme, whereby the interaction of the free solute with its environment (left leg) and with its counterpart in the dimer (right leg) is progressively turned out, viz. $\Delta G_{bind} = \Delta G^1_{annihil} - \Delta G^2_{annihil}$. Noteworthily, the left-hand side contribution, $\Delta G^1_{annihil}$, corresponds to the solvation free energy of quercetin, the determination of which is outlined in Figure 2.

To improve the precision of the estimates, the calculations in each solvent were run bidirectionally, and the free energy was obtained employing the Bennett acceptance ratio (BAR) method,[30] from whence a statistical error was inferred.[31] In general, the statistical error associated with this variance is somewhat smaller than the root mean-square deviation (rmsd) inferred from the free-energy estimates that were measured independently. Furthermore, to enhance the accuracy of the estimates,[28] in relation to finite-sampling biases, each bidirectional measure was conducted five times. The solvation free energies reported in the Results and Discussion correspond to the averages over the five realizations, and their reliability to the root-mean-square deviation (rmsd) thereof. Given the limited cost of the individual free-energy calculations, no specific attempt has been made here to optimize the computational effort against the accuracy of the free-energy estimates. Whereas reducing the number of bidirectional simulations to a lesser, albeit still reasonable number of independent observables, viz., typically three instead of five, would marginally decrease the precision of the estimate, it is strongly recommended, to perform the free-energy calculations bidirectionally to guarantee acceptably low statistical errors.[32]

The binding, or dimerization, free energies of quercetin were also measured in the different solvents, usng the FEP method, based on the thermodynamic cycle shown in Figure 3.

To reach this goal, a double-annihilation scheme was employed, whereby the interaction of the solute with its environment is obliterated in the free and in the bound states. It is worth noting that the first contribution to the binding affinity is equal to the solvation free energy determined previously. The sampling and stratification strategies are identical to that employed for determining solvation free energies. Although it would be desirable to provide BAR estimates, as was done for

TABLE 1: Experimental and Calculated Solubilities (c, mol/L) at 323 K of Quercetin in Chloroform, Water, Acetonitrile, Acetone, and *tert*-Amyl Alcohol[a]

	chloroform	water	acetonitrile	acetone	*tert*-amyl alcohol
log c_{exp}	insoluble[b]	−4.52[b]	−2.27[c]	−1.10[c]	−1.17[c]
ΔG_{solv}	−18.44 ± 0.18	−23.52 ± 0.19	−27.52 ± 0.28	−28.99 ± 0.38	−28.88 ± 0.26
log c_{calc}	−8.02	reference	−1.82	−0.81	−0.89
	−8.43	−4.98	reference	−1.27	−1.34
	−8.25	−4.80	−2.09	reference	−1.17
	−8.26	−4.81	−2.10	−1.10	reference
ΔG_{bind}	−3.47 ± 1.17	−6.00 ± 0.93	−1.88 ± 0.87	dissociated	dissociated

[a] c_{calc} is inferred according to eq 2 using successively the experimental solubility determined in each environment as a reference and the free energies of solvation (ΔG_{solv}, kcal/mol) computed using the FEP method. The binding free energies (ΔG_{bind}, kcal/mol) for the dimer of quercetin are also reported. [b] Determined using the same protocol as in Chebil et al.[12] [c] From Chebil et al.[12]

solvation energies, bidirectional simulations impose that restraints be enforced[33] as quercetin is created in the bound state, thereby guaranteeing the formation of the relevant noncovalent interactions. The contribution of these restraints to the binding affinity should in turn be evaluated, which constitute a potential additional source of error. Instead, to improve the accuracy of the estimates, annihilation of the solute was performed in ten independent simulations, from whence an average free energy was inferred, with an rmsd.

The free energy of solvation at a temperature T for any compound can be related to its solubility (c) through

$$c = c_A \exp\left(-\frac{\Delta G_{solv}}{RT}\right) \quad (2)$$

where c_A is the solubility of the pure crystal matter at T. It does not depend on the solvent, thereby allowing the solubilities measured in two different media to be connected via

$$c_2 = c_1 \exp\left(-\frac{\Delta G_{solv2} - \Delta G_{solv1}}{RT}\right) \quad (3)$$

From this equation, it is apparent that the solubility of a given compound can be inferred in any solvent on the basis of the knowledge of a solubility of reference in another solvent, together with the relevant free energies of solvation.

Results and Discussion

In this contribution, the solvation of quercetin is investigated in different media, e.g., water, acetonitrile, acetone, *tert*-amyl alcohol (2-methyl-2-butanol), and chloroform. The experimental solubility of quercetin varies dramatically with these solvents,[12] as can be seen in Table 1. Quercetin is not or is poorly soluble in chloroform, water, and acetonitrile. On the contrary, its solubility is rather high in acetone and *tert*-amyl alcohol, two solvents markedly amphiphilic.

The free energies of solvation (ΔG_{solv}) computed in this work (see Table 1) are consistent with the experimental solubility scale for quercetin, i.e., chloroform < water < acetonitrile < *tert*-amyl alcohol ≈ acetone, with values ranging from ca. −18 to −29 kcal/mol.

The experimental solubility in each media was used successively as a reference to estimate the solubility (c_{calc}) in the remaining solvents. The predicted solubilities reported in Table 1 are all within 0.5 log unit of the corresponding experimental values, irrespective of the reference solvent. Their reliability embraces three contributions (i) the accuracy of the experimental reference solubility, (ii) the relevance of the force field for the description of quercetin-solvent interactions, and (iii) both the precision and the accuracy of the computed solvation free energies. For the first contribution, the larger the solubility, the greater the accuracy. It is, therefore, desirable to have a high reference solubility to guarantee the lowest possible deviation between the predicted and the experimental values. As reported in Table 1, the largest errors for c_{calc} are observed when the low aqueous solubility of quercetin, $(2.98 \pm 0.31) \times 10^{-5}$ mol/L, is used as the reference solubility. Insofar as the force-field contribution is concerned, a reasonable description of electrostatic solute−solvent interactions was achieved by means of distinct sets of atomic charges assumed to account for the polarization of quercetin in the different media in an average sense (see Supporting Information). Finally, the strategy em-

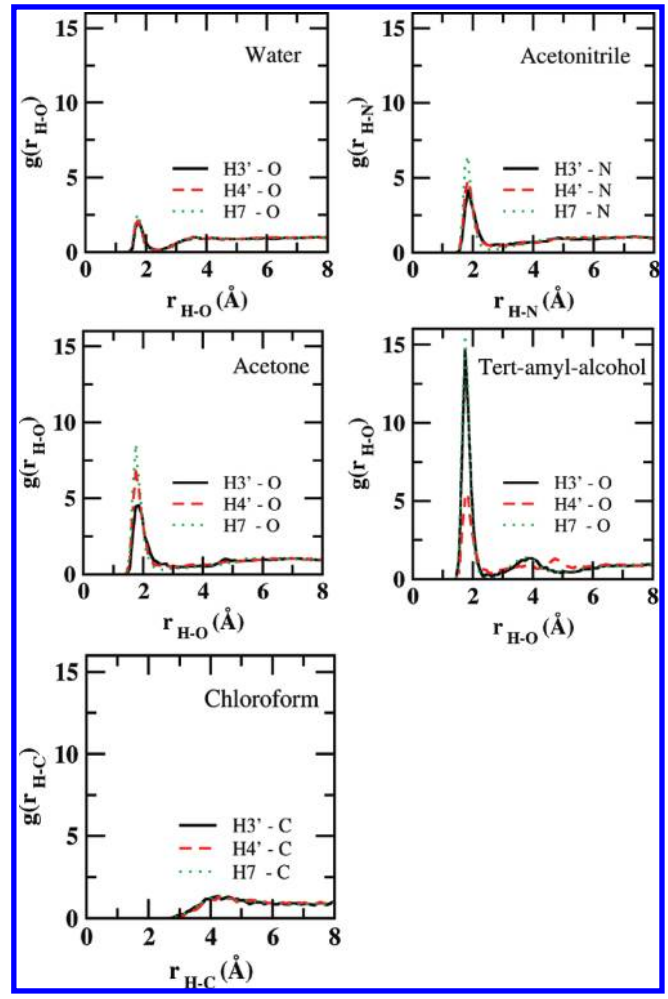

Figure 4. Radial distribution functions for hydroxyl moieties of quercetin and solvents.

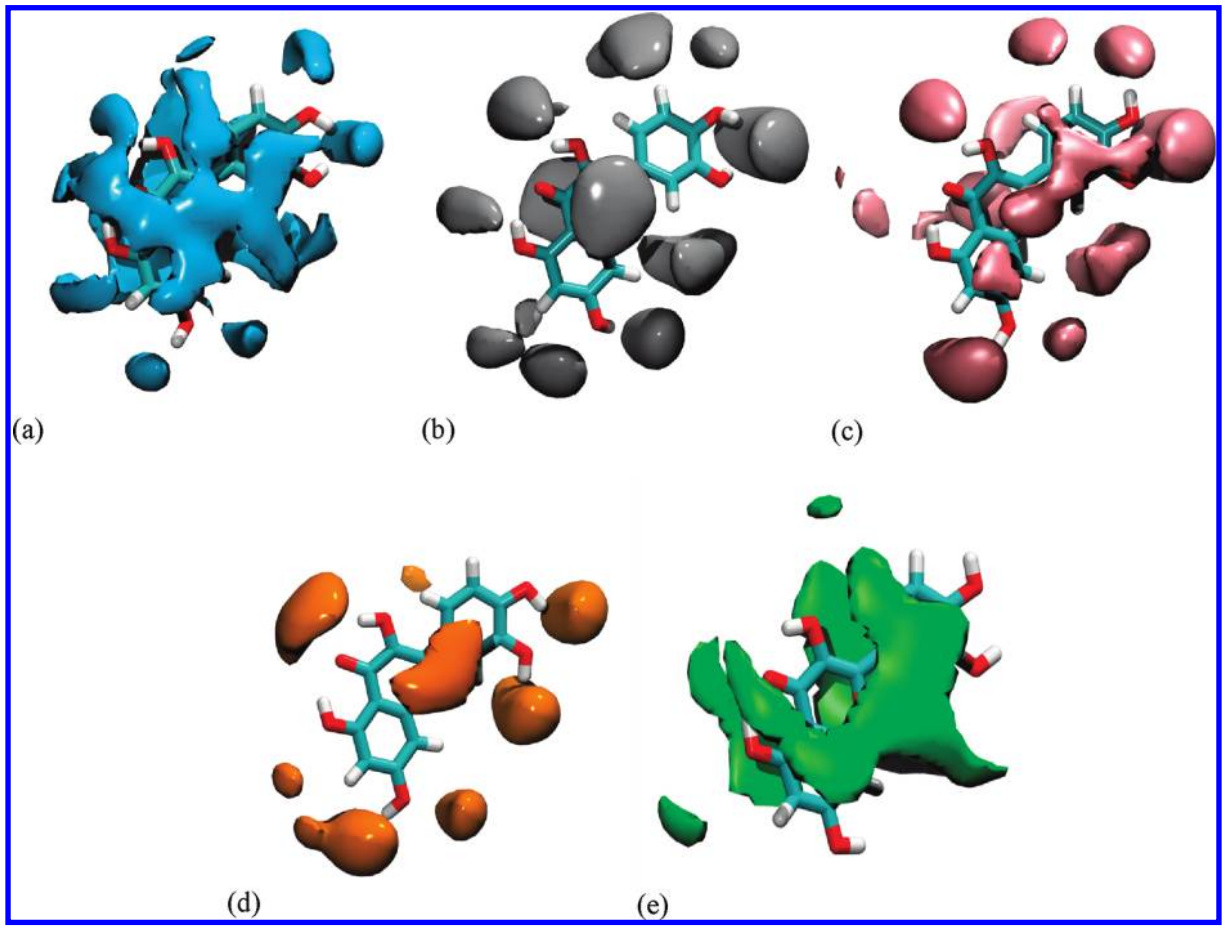

Figure 5. Contour maps of the solvent density around quercetin: (a) water; (b) acetonitrile; (c) acetone; (d) *tert*-amyl alcohol; (e) chloroform.

ployed herein allowed free energies of solvation to be determined with a root-mean-square deviation of less than 0.4 kcal/mol. That the free-energy estimates were obtained within chemical accuracy stems primarily from an appropriate sampling strategy together with the use of the Bennett acceptance ratio (BAR) method.[30] While both the statistical error and the rmsd are less than k_BT, this result is suggestive that a small bias arising from the finite length of the simulations may exist. This bias, which is related to the overall accuracy of the free-energy calculations, is mirrored in the generally appropriate, albeit occasionally imperfect, overlap of the underlying probability distributions for the forward and backward transformations (see Supporting Information).

The procedure utilized here not only provides a reliable prediction of the solubility but also gives access to the atomic detail of the solvation process, which is anticipated to help rationalize the solvent dependence of quercetin solubility. The pair distribution functions (see Figure 4) reveal different solvation patterns for the hydroxyl moieties at positions 3′, 4′, and 7 as a function of the environment. Not too surprisingly, there is no specific organization of chloroform around these hydrophilic groups. Water molecules are only marginally better organized around quercetin, which can be ascribed to the bulky hydrophobic core of the solute. In sharp contrast, amphipathic solvents are capable of interacting concomitantly with both the hydrophobic and the hydrophilic moieties of quercetin, reflected in a steadier organization of the solvent molecules around the solute.

A glance at the probability distributions of Figure 5 suggests, however, that the enhanced solvation of quercetin by acetone and *tert*-amyl alcohol stems from more pronounced hydrophobic and hydrophilic interactions, respectively, compared to the case for acetonitrile.

Interestingly enough, this information provides an additional rational for the optimization of the environment with the goal to increase the solubility of the substrate. In the case of quercetin, a more effective solvent would share the hydrophilic and hydrophobic moieties of *tert*-amyl-alcohol and acetone, respectively. Among other solvents, propan-2-ol meets these criteria. Not too surprisingly, the solubility of quercetin measured in this medium, following the procedure detailed in Chebil et al.,[12] proves to be larger, ∼29 g/L, than the corresponding concentration in *tert*-amyl-alcohol (∼20 g/L) and acetone (∼24 g/L).

To delve further into the solubility of quercetin and the role exerted by the solvent on this process, the dimerization free energy of the solute was measured in the different environments detailed above, as a putative model for the prediction of relative solubilities. As has been shown in the case of cyclodextrins,[34] this route constitutes a rudimentary and certainly incomplete approach toward the estimation of solubilities, although it provides valuable information on the propensity of the corresponding solid to dissociate. Here, simulations at thermodynamic equilibrium in *tert*-amyl alcohol and acetone have led in a systematic fashion to the dissociation of quercetin dimers, consistently with the high solubility in these two solvents. Conversely, a dimerization or binding free energy was measured in water, chloroform, and acetonitrile, following the thermodynamic cycle depicted in Figure 3. At the qualitative level, the nature of the environment yields distinct binding modes (see Supporting Information), hence resulting in dimerization free energies of different magnitudes. Specifically, a robust stacking

motif of quercetin is observed consistently in an aqueous medium. In sharp contrast, the hydrophobic environment of chloroform promotes the formation of dimers loosely bound by a few intermolecular hydrogen bonds and characterized by an appreciable configurational entropy. An intermediate behavior is found in the case of acetonitrile, where a large spectrum of binding motifs is observed, among which are short-lived, stacked, and hydrogen-bonded arrangements. At the quantitative level, the rmsd inferred from the ten independent free-energy calculations is significantly larger than any individual measure of the unidirectional statistical error.[28] To a large extent, this result can be understood by considering the configurational entropy of the dimers, which can hardly be embraced precisely in insufficiently long simulations. Binding free energies have, nonetheless, been estimated with a sufficient accuracy, allowing the different environments to be compared. The absolute value of the free energy of dimerization in acetonitrile is lower than the corresponding estimates in water and chloroform, which is consistent with the higher solubility of quercetin observed in this environment (see Table 1). On the contrary, the dimer model demonstrates to be insufficient to predict the lowest solubility of quercetin in chloroform ($\Delta G_{\text{bind}} = -3.47$ kcal/mol) compared to that in water ($\Delta G_{\text{bind}} = -6.00$ kcal/mol). Clearly, the precise estimation of the solid contribution to the solubility requires that complete models be employed to account for the overall interactions in the crystal, as devised by Lüder et al.,[6] who stated that the free energy required to extract one molecule out of the crystal is certainly different than that necessary to dissociate an isolated dimer.

Conclusion

In silico prediction of solubilities represents a challenging task for computational chemistry, which is in large measure connected with the difficulty to estimate the crystal contribution. Here, demonstration is made that accurate solubilities can be inferred for a wide range of environments at the price of minimal experimental input. The strategy put forth requires the knowledge of a unique experimental solubility together with a set of free energies of solvation. The latter quantities can be computed within chemical accuracy, as illustrated in the case of quercetin in chloroform, water, acetonitrile, acetone, and *tert*-amyl alcohol. In the context of pharmaceutical high-throughput screening, it might be advantageous to consider alternatives to free-energy perturbation, like quantum-mechanical calculations relying on a polarizable continuum description, which are unquestionably faster but also offer a less detailed and somewhat more approximate picture of solvation phenomena.[35] Regardless of the experimental reference, the solubilities were determined within 0.5 log unit. Combined with the current arsenal of tools available to the computational chemist, the present methodology is envisioned to help predict solubilities in a more routine fashion and to constitute a milestone on the road toward the rational design and synthesis of novel molecular compounds.

Supporting Information Available: Atomic charges for quercetin in each solvent. Potential energy surface as a function of φ. Quercetin dimer geometries. Probability distributions underlying the annihilation and creation transformations of quercetin in acetonitrile. This material is available free of charge via the Internet at http://pubs.acs.org.

References and Notes

(1) Huuskonen, J.; Livingstone, D. J.; Manallack, D. T. Prediction of drug solubility from molecular structure using a drug-like training set. *SAR QSAR Environ. Res.* **2008**, *19*, 191–212.

(2) Zheng, Y.; Mo, Q.; Liu, Z. The studies of QSPR/QSAR for ionic liquids. *Prog. Chem.* **2009**, *21*, 1772–1781.

(3) Obrezanova, O.; Gola, J. M. R.; Champness, E. J.; Segall, M. D. Automatic QSAR modeling of ADME properties: Blood-brain barrier penetration and aqueous solubility. *J. Comput.-Aided Mol. Des.* **2008**, *22*, 431–440.

(4) Westergren, J.; Lindfors, L.; Höglund, T.; Lüder, K.; Nordholm, S.; Kjellander, R. In silico prediction of drug solubility: 1. Free energy of hydration. *J. Phys. Chem. B* **2007**, *111*, 1872–1882.

(5) Lüder, K.; Lindfors, L.; Westergren, J.; Nordholm, S.; Kjellander, R. In silico prediction of drug solubility: 2. Free energy of solvation in pure melts. *J. Phys. Chem. B* **2007**, *111*, 1883–1892.

(6) Lüder, K.; Lindfors, L.; Westergren, J.; Nordholm, S.; Kjellander, R. In silico prediction of drug solubility. 3. Free energy of solvation in pure amorphous matter. *J. Phys. Chem. B* **2007**, *111*, 7303–7311.

(7) Lüder, K.; Lindfors, L.; Westergren, J.; Nordholm, S.; Persson, R.; Pedersen, M. In Silico prediction of drug solubility: 4. Will simple potentials suffice. *J. Comput. Chem.* **2009**, *30*, 1859–1871.

(8) Zwanzig, R. W. High-temperature equation of state by a perturbation method. I. Nonpolar gases. *J. Chem. Phys.* **1954**, *22*, 1420–1426.

(9) Havsteen, B. H. The biochemistry and medical significance of the flavonoids. *Pharmacol. Therapeut.* **2002**, *96*, 67–202.

(10) Heim, K. E.; Tagliaferro, A. R.; Bobilya, D. J. Flavonoid antioxidants: chemistry, metabolism and structure-activity relationships. *J. Nutr. Biochem.* **2002**, *13*, 572–584.

(11) Chebil, L.; Anthoni, J.; Humeau, C.; Gerardin, C.; Engasser, J. M.; Ghoul, M. Enzymatic acylation of flavonoids: effect of the nature of substrate, origin of lipase and operating conditions on conversion yield and regioselectivity. *J. Agric. Food Chem.* **2007**, *55*, 9496–9502.

(12) Chebil, L.; Humeau, C.; Anthony, J.; Dehez, F.; Engasser, J. M.; Ghoul, M. Solubility of flavonoids in organic solvents. *J. Chem. Eng. Data* **2007**, *52*, 1552–1556.

(13) Jorgensen, W. L.; Maxwell, D. S.; Tirado-Rives, J. Development and testing of the OPLS all-atom force field on conformational energetics and properties of organic liquids. *J. Am. Chem. Soc.* **1996**, *118*, 11225–11236.

(14) Jorgensen, W. L.; Chandrasekhar, J.; Madura, J. D.; Impey, R. W.; Klein, M. L. Comparison of simple potential functions for simulating liquid water. *J. Chem. Phys.* **1983**, *79*, 926–935.

(15) Grabuleda, X.; Jaime, C.; Kollman, P. A. Molecular dynamics simulation studies of liquid acetonitrile: new six-site model. *J. Comput. Chem.* **2000**, *21*, 901–908.

(16) Price, M. L. P.; Ostrovsky, D.; Jorgensen, W. L. Gas-phase and liquid-state properties of esters, nitriles, and nitro compounds with the OPLS-AA force field. *J. Comput. Chem.* **2001**, *22*, 1340–1352.

(17) Martin, M. G.; Biddy, M. J. Monte Carlo molecular simulation predictions for the heat of vaporization of acetone and butyramide. *Fluid Phase Equilib.* **2005**, *236*, 53–57.

(18) Jorgensen, W. L.; Briggs, J. M.; Contreras, M. L. Relative partition coefficients for organic solutes from fluid simulations. *J. Phys. Chem.* **1990**, *94*, 1683–1686.

(19) Lee, C.; Yang, W.; Parr, R. G. Development of the Colle-Salvetti correlation-energy formula into a functional of the electron density. *Phys. Rev. B* **1988**, *37*, 785–789.

(20) Frisch, M. J.; Trucks, G. W.; Schlegel, H. B.; Scuseria, G. E.; Robb, M. A.; Cheeseman, J. R.; Montgomery, J. A.; Vreven, J. T.; Kudin, K. N.; Burant, J. C.; Millam, J. M.; Iyengar, S. S.; Tomasi, J.; Barone, V.; Mennucci, B.; Cossi, M.; Scalmani, G.; Rega, N.; Petersson, G. A.; Nakatsuji, H.; Hada, M.; Ehara, M.; Toyota, K.; Fukuda, R.; Hasegawa, J.; Ishida, M.; Nakajima, T.; Honda, Y.; Kitao, O.; Nakai, H.; Klene, M.; Li, X.; Knox, J. E.; Hratchian, H. P.; Cross, J. B.; Bakken, V.; Adamo, C.; Jaramillo, J.; Gomperts, R.; Stratmann, R. E.; Yazyev, O.; Austin, A. J.; Cammi, R.; Pomelli, C.; Ochterski, J. W.; Ayala, P. Y.; Morokuma, K.; Voth, G. A.; Salvador, P.; Dannenberg, J. J.; Zakrzewski, V. G.; Dapprich, S.; Daniels, A. D.; Strain, M. C.; Farkas, O.; Malick, D. K.; Rabuck, A. D.; Raghavachari, K.; Foresman, J. B.; Ortiz, J. V.; Cui, Q.; Baboul, A. G.; Clifford, S.; Cioslowski, J.; Stefanov, B. B.; Liu, G.; Liashenko, A.; Piskorz, P.; Komaromi, I.; Martin, R. L.; Fox, D. J.; Keith, T.; Al-Laham, M. A.; Peng, C. Y.; Nanayakkara, A.; Challacombe, M.; Gill, P. M. W.; Johnson, B.; Chen, W.; Wong, M. W.; Gonzalez, C.; Pople, J. A. *Gaussian 03*, Revision C.02; Gaussian, Inc.: Wallingford, CT, 2004.

(21) Tomasi, J.; Persico, M. Molecular interactions in solution: An overview of methods based on continuous distributions of the solvent. *Chem. Rev.* **1994**, *94*, 2027–2094.

(22) Ángyán, J. G.; Chipot, C.; Dehez, F.; Hätting, C.; Jansen, G.; Millot, C. OPEP. A tool for the optimal partitioning of electric properties. *J. Comput. Chem.* **2003**, *24*, 997–1008.

(23) Phillips, J. C.; Braun, R.; Wang, W.; Gumbart, J.; Tajkhorshid, E.; Villa, E.; Chipot, C.; Skeel, R. D.; Kale, L.; Schulten, K. Scalable molecular dynamics with NAMD. *J. Comput. Chem.* **2005**, *26*, 1781–1802.

(24) Feller, S. E.; Zhang, Y.; Pastor, R. W.; Brooks, B. R. Constant pressure molecular dynamics simulation: The Langevin piston method. *J. Chem. Phys.* **1995**, *103*, 4613–4621.

(25) Darden, T. Y., D.; Pedersen, L. Particle mesh Ewald: An N•log(N) method for Ewald sums in large systems. *J. Chem. Phys.* **1993**, *98*, 10089–10092.

(26) Tuckerman, M.; Berne, B. J.; Martyna, G. J. Reversible multiple time scale molecular dynamics. *J. Chem. Phys.* **1992**, *97*, 1990–2001.

(27) Gilson, M. K.; Given, J. A.; Bush, B. L.; McCammon, J. A. The statistical-thermodynamic basis for computation of binding affinities: A critical review. *Biophys. J.* **1997**, *72*, 1047–1069.

(28) Chipot, C.; Pohorille, A. *Free energy calculations. Theory and applications in chemistry and biology*; Springer Verlag: Berlin, Heidelberg, 2007

(29) Zacharias, M.; Straatsma, T. P.; McCammon, J. A. Separation-shifted scaling, a new scaling method for Lennard-Jones interactions in thermodynamic integration. *J. Chem. Phys.* **1994**, *100*, 9025–9031.

(30) Bennett, C. H. Efficient estimation of free energy differences from Monte Carlo data. *J. Comput. Phys.* **1976**, *22*, 245–268.

(31) Hahn, A. M.; Then, H. Characteristic of Bennett's acceptance ratio method. *Phys. Rev. E: Stat. Nonlinear Soft Matter Phys.* **2009**, *80*, 031111.

(32) Pohorille, A.; Jarzynski, C.; Chipot, C. Good practices in free-energy calculations. *J. Phys. Chem. B* **2010**, *114*, 10235−10253.

(33) Deng, Y.; Roux, B. Computations of standard binding free energies with molecular dynamics simulations. *J. Phys. Chem. B* **2009**, *113*, 2234–2246.

(34) Cai, W.; Sun, T.; Shao, X.; Chipot, C. Can the anomalous aqueous solubility of β-cyclodextrin be explained by its hydration free energy alone. *Phys. Chem. Chem. Phys.* **2008**, *10*, 3236–3243.

(35) Orozco, M.; Luque, F. J. Theoretical methods for the description of the solvent effect in biomolecular systems. *Chem. Rev.* **2000**, *100*, 4187–4226.

JP104569K